

Nickel Oxide Particles Coated with Silica

Satoshi Sato,* Ryoji Takahashi, Toshiaki Sodesawa, Nobuyuki Ichikuni, and Hidefumi Amano

Department of Materials Technology, Faculty of Engineering, Chiba University, Yayoi, Inage, Chiba 263-8522

(Received May 14, 2002)

Fine particles of SiO_2-coated Ni metal were prepared by depositing silica on a $Ni(OH)_2$ precipitate in a dissolution–deposition process of silica glass under hydrothermal conditions, followed by calcination and reduction. A fresh precipitate of $Ni(OH)_2$ was heated with a NaOH solution containing several pieces of silica glass chips in a pressure vessel at 100 °C. Silica components dissolved from the glass chips were deposited on the $Ni(OH)_2$ precipitate, and the silica loading increased with increasing the hydrothermal period. Even after calcination at 500 °C, a specific surface area of the resulting SiO_2–NiO increased with silica loading, and exceeded 200 $m^2\ g^{-1}$. SiO_2–NiO, reduced at 500 °C, had a metal surface area as high as 22 $m^2\ g^{-1}$. In contrast to the fact that pure $Ni(OH)_2$ readily aggregates during heating, the SiO_2-coated $Ni(OH)_2$ particles are protected from agglomerating during the hydrothermal process, calcination, and reduction.

It is known that amorphous silica is dissolved in aqueous alkaline solution.[1–3] Both the dissolution rate and the solubility of silica increase with increasing pH of the solution[2] and temperature.[3] We have recently found that silica dissolved in an aqueous ammonia solution deposits on precipitates of $ZrO(OH)_2$ under hydrothermal (HT) conditions at 100 °C.[4] The deposited silica prevents the agglomeration of particles during calcination: a high specific surface area of the precipitate is retained even after calcination. The specific surface area exceeds 240 $m^2\ g^{-1}$ in the SiO_2–ZrO_2 sample calcined at 500 °C.

In vapor-phase deposition processes,[5–9] SiO_2–Al_2O_3, SiO_2–ZrO_2 and SiO_2–TiO_2 have been prepared by depositing silica on the supports using silicon alkoxide. In the vapor-phase process, oxide supports limit the specific surface area of the resulting composite material: the specific surface area of ZrO_2 and TiO_2 supports is less than 70 $m^2\ g^{-1}$,[8,9] and that of alumina is 200 $m^2\ g^{-1}$.[5–7] In contrast to the vapor-phase deposition process, the HT process has an advantage in depositing silica, because the deposition proceeds under mild conditions without loosing the high surface area of the precursor metal hydroxides. We expect that the dissolution-deposition nature of silica in a basic solution under HT conditions would have some probability for the preparation of fine particles of other SiO_2-coated metal oxides.

In preliminary tests, we examined the treatment of several metal hydroxides in a basic solution with silica glass chips under HT conditions. No silica deposition, however, occurred upon the hydroxides of Al(III) and Ti(IV) at pH = 10.[4] The isoelectric point of aluminum hydroxide is close to the pH of the deposition conditions.[10] We speculate that the bonds of Si–O–Al and Si–O–Ti are unstable near the isoelectric points. In contrast, we have found that silica deposits on such hydroxides of metals as Ni(II) and Sn(IV) in an aqueous basic solution at a pH of ca. 10.

In this paper, we examine the deposition behavior of silica on a $Ni(OH)_2$ precipitate in a sodium hydroxide solution under HT conditions and the structure of the resulting SiO_2-coated $Ni(OH)_2$ and a calcined body of SiO_2-coated NiO. We also consider the reduction of SiO_2–NiO and the surface structure of the reduced SiO_2–NiO.

Experimental

Sample Preparation. All reagents were supplied by Wako Pure Chemical Industry Ltd. (Japan). A precipitate of $Ni(OH)_2$ was obtained by adding 10 wt% of a $Ni(NO_3)_2$ solution into 1.0 mol dm^{-3} of a NaOH solution (100 cm^3). After filtration and removal of NaOH by washing the precipitate, it was used for the following HT process. The precipitate with a Ni content of 13.5 mmol was placed in a poly(tetrafluoroethylene) vessel together with 25 cm^3 of a 0.02–0.5 mol dm^{-3} NaOH solution, and was heated at 100 °C for 12–336 h in a 50 cm^3 pressure vessel. In the HT process for silica deposition, several pieces of silica glass tube (SiO_2 content, 100%; outside diameter, 6 mm; inside, 4 mm; length, 20–40 mm) with the total surface area adjusted to ca. 190 cm^2 were immersed in the solution. The precipitate was washed with distilled water and dried at 110 °C for 24 h to obtain a SiO_2–$Ni(OH)_2$ sample. Then, it was calcined in air at 500 °C for 3 h at a heating rate of 1 K min^{-1} to obtain a SiO_2–NiO sample.

Characterization. A specific surface area (abbreviated to SA) of the sample was determined by the BET method using the N_2 adsorption isotherm at −196 °C measured with a conventional volumetric gas adsorption apparatus. Prior to adsorption, the dried and calcined samples were heated in a vacuum at 110 and 300 °C for 1 h, respectively. According to a method reported by Dollimore and Heal,[11] the pore-size distribution was calculated using the desorption branch of the N_2 adsorption-desorption isotherm at −196 °C, measured by Omnisorp 100CX (Coulter, U.S.A.).

XRD profiles of samples were recorded on an M18XHF (Mac Science, Japan). Transmission electron micrograph (TEM) images were observed on a JEM-4000 FXII (JEOL, Japan) instrument operated at 400 kV. Powder samples pipetted onto a copper microgrid with collodion film from their suspension in acetone were

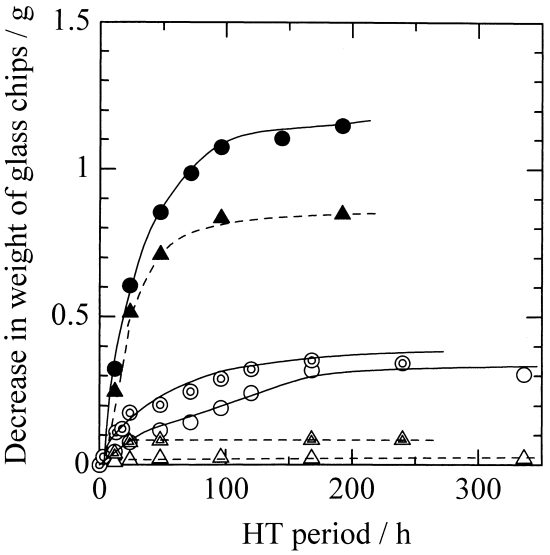

Fig. 1. Changes in decrease in weight of glass chips during HT process. ○, △, heated in 0.02 mol dm^{-3} NaOH solution; ◎, ◬, 0.05 mol dm^{-3}; ●, ▲, 0.5 mol dm^{-3}; circles, under HT conditions with $Ni(OH)_2$; triangles, without $Ni(OH)_2$.

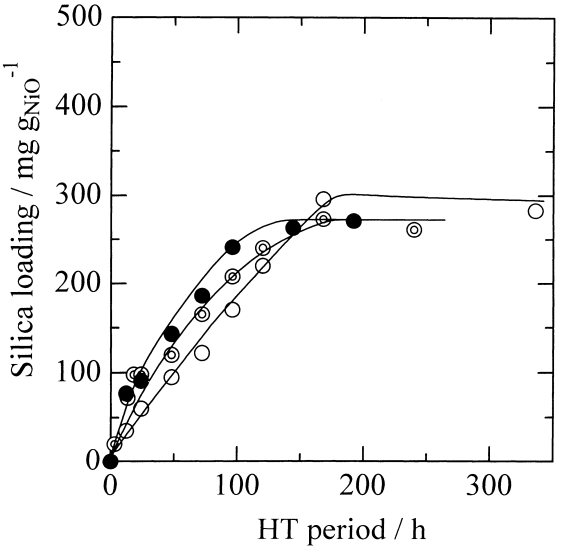

Fig. 2. Changes in silica loading with HT period. (○), heated in 0.02 mol dm^{-3} NaOH solution; (◎), 0.05 mol dm^{-3}; (●), 0.5 mol dm^{-3}.

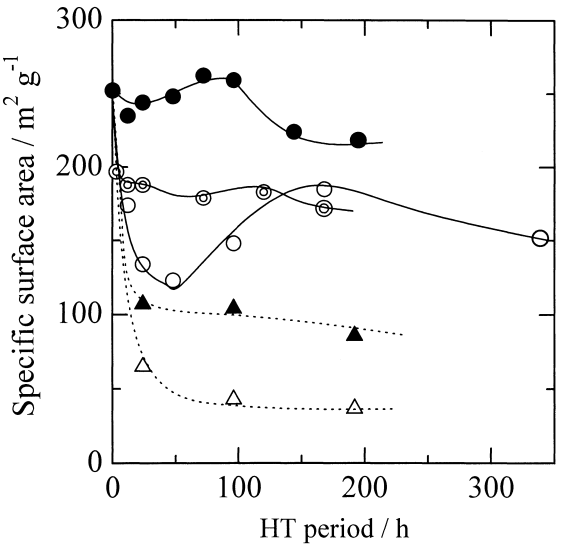

Fig. 3. Changes in the specific surface areas of SiO_2–$Ni(OH)_2$ with HT period. The sample was dried at 110 °C for 24 h. ○, △, heated in 0.02 mol dm^{-3} NaOH solution; ◎, 0.05 mol dm^{-3}; ●, ▲, 0.5 mol dm^{-3}; circles, under HT conditions with silica; triangles, without silica.

used for TEM observations.

A temperature-programmed reduction (TPR) profile was measured from 30 to 900 °C at a heating rate of 5 K min^{-1} with a hand-made apparatus. A catalyst sample (ca. 25 mg) was fixed in a quartz glass tube with quartz glass wool. A mixture of H_2/N_2 (= 1/9) was flowed at atmospheric pressure at a flow rate of 10 cm^3 min^{-1}, and the consumption of H_2 was detected by a thermal-conductivity detector.[12,13]

The Ni metal surface area of reduced sample was determined by hydrogen chemisorption at 0 °C in a conventional volumetric gas adsorption apparatus. Prior to the measurement, the sample was reduced by hydrogen under an initial pressure of 39.5 kPa at 500 °C for 2 h. Details of the procedure are described elsewhere.[14]

Results

Silica Deposition on $Ni(OH)_2$. Figure 1 shows the changes in the amount of silica dissolved with the HT period at different NaOH concentrations. The simple dissolution of silica was not negligible in 0.05 and 0.5 mol dm^{-3} of NaOH solution at 100 °C, even in the absence of $Ni(OH)_2$, whereas it was negligible in the HT process at a low concentration of 0.02 mol dm^{-3}. The difference in the amount of silica dissolved under conditions between the presence and absence of $Ni(OH)_2$ precipitate is regarded as silica loading. Silica loading increases with increasing HT period, and is saturated with the loading of ca. 300 mg g_{NiO}^{-1} at any NaOH concentration after 150 h (Fig. 2). During short HT periods within 100 h, the silica loading at high NaOH concentration is larger than that at low concentration.

Figure 3 shows the changes in SA of SiO_2–$Ni(OH)_2$ prepared at different concentrations of NaOH solution with the HT period. In the absence of silica glass during the HT process, SA of $Ni(OH)_2$ dried at 110 °C decreased steeply within 24 h at any NaOH concentration. In contrast, the samples treated with silica retained high SA values. At a high NaOH concentration of 0.5 mol dm^{-3}, the high SA of the sample dried at 110 °C was maintained with a slight decrease with increasing HT period. At a low concentration of 0.02 mol dm^{-3}, the SA value decreased with the HT period minimizing at 48 h, and then increased while showing a maximum at 168 h. At a medium concentration of 0.05 mol dm^{-3}, the SA value decreased monotonously with increasing the HT period.

Structure of Silica-Deposited NiO. Figure 4 shows the changes in SA of SiO_2–NiO calcined at 500 °C. In the absence of silica glass during the HT process, SA of pure NiO is almost constant at as low as 30 m^2 g^{-1} irrespective of the HT period.

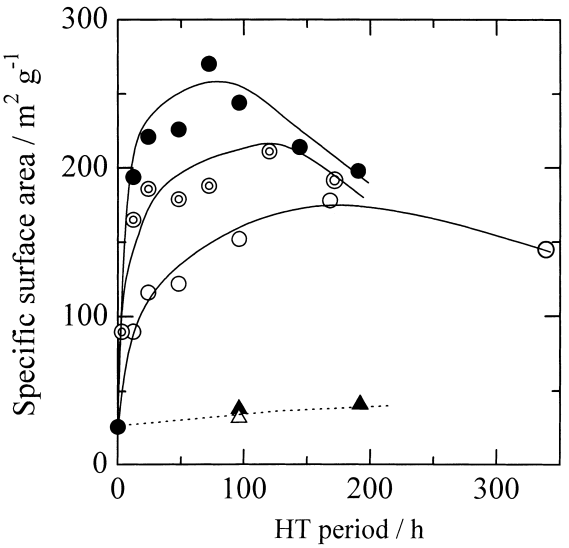

Fig. 4. Changes in the specific surface areas of SiO_2–NiO with HT period. The sample was calcined at 500 °C for 3 h. Symbols are the same as those in Fig. 3.

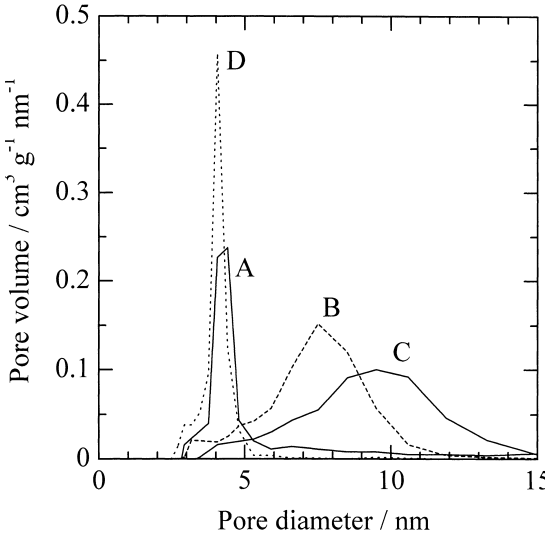

Fig. 5. Pore size distribution of SiO_2–NiO treated with different NaOH concentration. (A) heated in 0.02 mol dm^{-3} NaOH aq for 168 h; (B) 0.5 mol dm^{-3} for 48 h; (C) 0.5 mol dm^{-3} for 144 h; (D) as-dried pure $Ni(OH)_2$ without HT process.

In the presence of silica glass, however, the SA value of SiO_2–NiO increases with increasing HT period at any NaOH concentration, and shows a maximum. Moreover, the SA of SiO_2–NiO is the same as that of SiO_2–$Ni(OH)_2$ for a HT period above 48 h, while it is smaller than the latter for a short HT period (Figs. 3 and 4).

Figure 5 depicts the pore-size distribution of SiO_2–NiO prepared at different NaOH concentrations. At a low NaOH concentration of 0.02 mol dm^{-3}, the sample has a pore-size distribution similar to that obtained in an as-dried $Ni(OH)_2$ sample without the HT process. The distribution shifts to a large pore size with increasing HT period at a high NaOH concentration of 0.5 mol dm^{-3}. The distribution is almost the same as that observed in a sample dried at 110 °C, except for the pure NiO, which looses the pore volume of as-dried $Ni(OH)_2$ during calcination at 500 °C (profiles not shown). Table 1 also summarizes the pore volume and peak top in the pore-size distribution for the SiO_2–$Ni(OH)_2$ and SiO_2–NiO samples.

Figure 6 depicts the XRD profiles of SiO_2–$Ni(OH)_2$ samples dried at 110 °C. The diffraction peaks at 2θ = 19.3, 33.1, 38.6, 52.2, 59.1, and 62.7 degrees are assigned as planes of (001), (100), (101), (102), (110), and (111) of layer-structured

Table 1. Physical Properties of Samples Prepared in Different NaOH Concentration at 100 °C[a)]

HT period/h	SiO_2 loading /mg g_{NiO}^{-1}	SA/m^2 g^{-1} [b)]			PV/cm^3 g^{-1} [b)]		PD/nm[c)]	
		dried	calcined	reduced	dried	calcined	dried	calcined
0	0	252	26	< 1	0.212	—	4.1	—
Prepared in 0.02 mol dm^{-3} NaOH solution								
12	35	174	90	54	—	0.030	—	4.1
48	95	123	122	95	0.287	0.255	4.2	4.4
96	170	148	152	117	0.282	0.275	4.2	4.4
168	296	185	178	163	0.288	0.327	4.4	4.5
Prepared in 0.05 mol dm^{-3} NaOH solution								
24	98	188	186	145	0.273	0.341	4.2	4.2
168	270	174	193	196	0.304	0.335	4.6	4.2
Prepared in 0.5 mol dm^{-3} NaOH solution								
24	91	244	221	178	0.315	0.388	4.2	6.6
48	143	248	226	205	0.360	0.430	6.1	7.5
144	263	224	214	145	0.486	0.502	8.5	9.5
192[d)]	0	86	41	—	0.220	—	8.5	—

a) samples dried at 110 °C (SiO_2–$Ni(OH)_2$), calcined at 500 °C (SiO_2–NiO), and reduced at 500 °C. b) specific surface area (SA) and pore volume (PV) obtained from N_2 adsorption isotherm measured at −196 °C. c) pore diameter (PD) shows peak top of the pore size distribution observed in Fig. 5. d) prepared under HT process in the absence of silica glass chips.

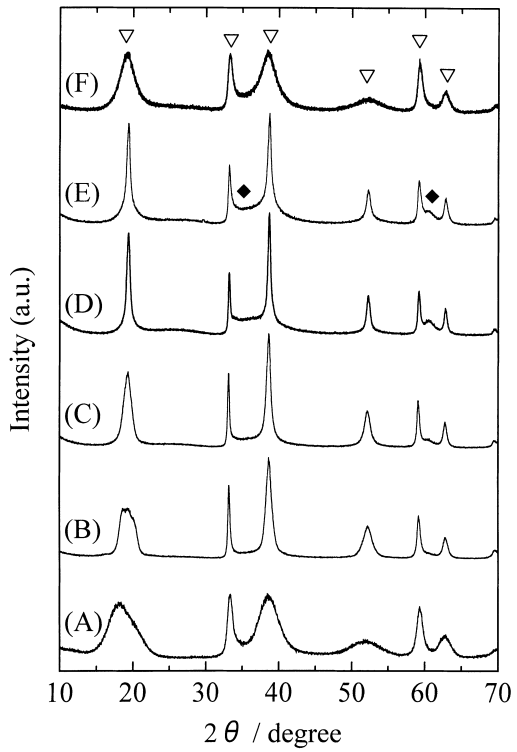

Fig. 6. XRD profiles of SiO_2–$Ni(OH)_2$ dried at 110 °C. (A) non-hydrothermal sample; (B) heated in 0.02 mol dm^{-3} NaOH aq for 48 h; (C) 96 h; (D) 168 h; (E) 0.05 mol dm^{-3} for 168 h; (F) 0.5 mol dm^{-3} for 144 h. ▽: $Ni(OH)_2$, ◆: Ni_2SiO_4.

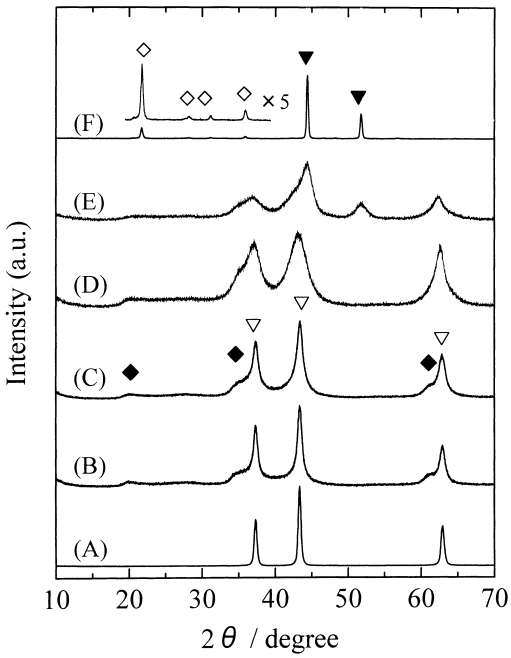

Fig. 7. XRD profiles of SiO_2–NiO calcined at 500 °C. (A) non-hydrothermal sample; (B) heated in 0.02 mol dm^{-3} NaOH aq for 168 h; (C) 0.05 mol dm^{-3} for 168 h; (D) 0.5 mol dm^{-3} for 144 h; (E) sample D reduced by H_2 at 500 °C for 3 h; (F) sample D reduced by H_2 at 800 °C for 3 h. ▽: NiO, ◆: Ni_2SiO_4, ▼: Ni, ◇: Na_2SiO_3.

α–$Ni(OH)_2$, respectively. Different sharpnesses of the diffraction peaks in each profile indicate that the $Ni(OH)_2$ crystallites have anisotropy. Each peak becomes sharper with the HT period. That is, the $Ni(OH)_2$ precipitate dose not change the crystalline phase, whereas it changes the crystallite size. In addition, small peaks observed at 2θ = ca. 35 and 61 degrees are ascribed to Ni_2SiO_4 for samples with large silica loading (Fig. 6, C–E).

Figure 7 depicts XRD profiles of SiO_2–NiO calcined at 500 °C. The major peaks of the NiO phase are observed at 2θ = 37.2, 43.3, and 62.9 degrees, which are assigned as planes of (111), (200), and (220), respectively, while the broad peaks of the nickel silicate phase are observed at 2θ = 19.9, 34.5, and 61.2 degrees. The diffraction peaks of NiO broaden with increasing NaOH concentration in the preparation. The particle size of $Ni(OH)_2$ and NiO with different plane directions is calculated by the Scherrer's equation (Table 2).

Figure 8 depicts TEM images of SiO_2–$Ni(OH)_2$ samples prepared at different NaOH concentrations. SiO_2–$Ni(OH)_2$ has different shapes: SiO_2–$Ni(OH)_2$ prepared at 0.02 mol dm^{-3} is composed of particles with spherical and rod shapes (Fig. 8A), but that at 0.5 mol dm^{-3} is composed of whiskers (Fig. 8B). In addition, the SiO_2–NiO samples without reduction (photo not shown) have the same figure as the reduced bodies, and their particle size is larger than that of the reduced ones.

Reduction of SiO_2–NiO. Figure 7 also contains XRD patterns of the SiO_2–NiO reduced at 500 and 800 °C. At 500 °C, a part of the NiO phase transforms into the Ni metal phase at 2θ = 44.4 and 51.8 degrees (Fig. 7E), while Ni_2SiO_4 is reduced to the Ni metal phase with the formation of Na_2SiO_3 at 800 °C (Fig. 7F). Na_2SiO_3 is observed in samples prepared at higher NaOH concentrations. A TEM photograph of SiO_2–NiO reduced at 500 °C is depicted in Fig. 8C. Diffraction from Ni metal is observed on the particles in the photograph. It is obvious that the sample consists of Ni particles. Every dark Ni metal particle is surrounded by a bright shell. The bright shell is caused not by a Fresnel fringe, but by amorphous materials. This shows that the dark Ni cores have core-shell structures covered by a bright silica shell.

Figure 9 shows TPR profiles of SiO_2–NiO. The pure NiO is readily reduced at 300–400 °C. With increasing silica loading, the reduction peak shifts to higher temperatures, and a broad peak appears between 500–800 °C. At the same silica loading level, the former peak decreases with increasing concentration of NaOH solution in the HT process, while the latter increases. This indicates that the samples prepared at higher NaOH concentrations and for a longer HT period are less reducible.

Because the reduced SiO_2–NiO chemisorbed hydrogen, a part of the Ni metal exposed its surface from a gap in the silica skin. Figure 10 shows the Ni metal surface area of the SiO_2–NiO reduced by H_2 at 500 °C. In samples prepared at different concentrations of NaOH solution in the HT process, the Ni metal surface areas vary with the HT period, and show maxima (Fig. 10). At a low concentration of 0.02 mol dm^{-3}, the Ni metal surface area is as high as 22 $m^2\ g^{-1}$. The value is as high as the Ni metal surface area reported for Ni–MgO prepared by a citrate process[12] and Ni–SiO_2 prepared through a sol-gel process of silicon alkoxide.[15,16]

Table 2. Particle Size of SiO_2–$Ni(OH)_2$ and SiO_2–NiO

HT period /h	SiO_2 loading /mg g_{NiO}^{-1}	Particle size/nm[a)]			
		SiO_2–$Ni(OH)_2$[b)]		SiO_2–NiO[b)]	
		(001) plane	(100) plane	(111) plane	(200) plane
0	0	2.4	11	20	20
Prepared in 0.02 mol dm^{-3} NaOH solution.					
12	35	4.6	20	17	21
24	60	4.4	26	17	15
48	95	3.7	27	15	14
96	170	7.3	30	14	13
168	296	16	30	13	12
24[c)]	0	4.3	13	19	20
Prepared in 0.05 mol dm^{-3} NaOH solution					
24	98	14	20	11	9.5
120	240	15	22	10	10
Prepared in 0.5 mol dm^{-3} NaOH solution					
48	143	4.4	12	5.4	4.1
144	263	4.4	12	4.4	3.7
24[c)]	0	7.7	20	—	—
192[c)]	0	24	23	16	15

a) calculated by Scherrer's equation. b) SiO_2–$Ni(OH)_2$ dried at 110 °C, SiO_2–NiO calcined at 500 °C. c) without using silica glass chips in HT process.

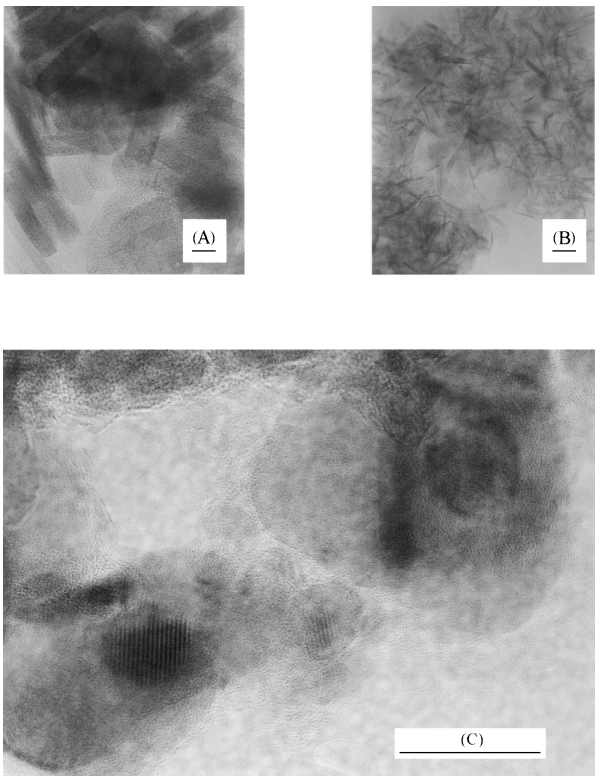

Fig. 8. TEM images of SiO_2–$Ni(OH)_2$ dried at 110 °C (A,B) and SiO_2–NiO reduced at 500 °C (C). (A) and (C) prepared with HT treatment in 0.02 mol dm^{-3} NaOH aq for 168 h, silica loading of 296 mg g_{NiO}^{-1}; (B) in 0.5 mol dm^{-3} NaOH aq for 144 h, 263 mg g_{NiO}^{-1}; (bar = 20 nm).

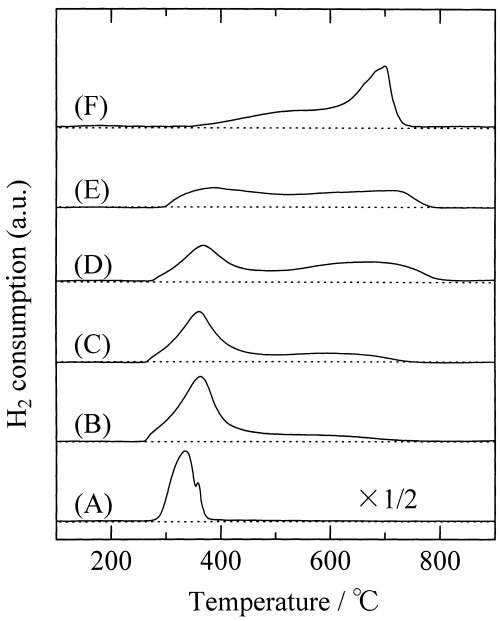

Fig. 9. TPR profiles of SiO_2–NiO calcined at 500 °C. (A) non-hydrothermal sample; (B) heated in 0.02 mol dm^{-3} NaOH aq for 48 h; (C) 96 h; (D) 168 h; (E) 0.05 mol dm^{-3} for 168 h; (F) 0.5 mol dm^{-3} for 144 h.

The SA values of the reduced SiO_2–NiO catalysts are also listed in Table 1. The reduction at 500 °C decreases the SA values to different extents. In samples prepared at a low NaOH concentration, the SA greatly decreases. Figure 11 shows the changes in the fraction of Ni metal surface area to SA of the reduced SiO_2–NiO. In samples prepared at a low NaOH concentration of 0.02 mol dm^{-3}, a large fraction of the Ni metal surface was found to be exposed.

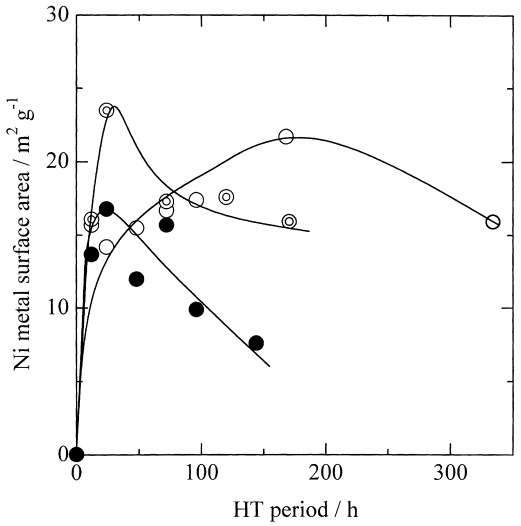

Fig. 10. Changes in Ni metal surface of SiO_2–NiO reduced at 500 °C with HT period. Symbols are the same as those in Fig. 2.

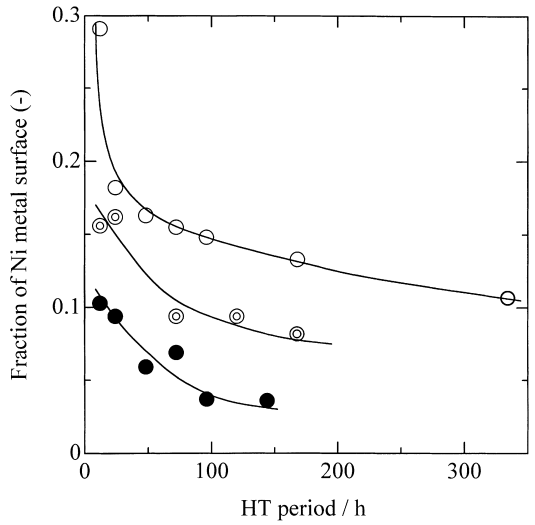

Fig. 11. Changes in fraction of Ni metal surface of SiO_2–NiO reduced at 500 °C. Symbols are the same as those in Fig. 2.

Discussion

Deposition of Silica. In a hydrothermal treatment in a NaOH solution, the silica glass chips decrease in weight irrespective of the presence of a $Ni(OH)_2$ precipitate, and the decrease in weight increases with increasing the HT period (Fig. 1). Although the dissolved silica is negligibly small at a NaOH concentration of 0.02 mol dm^{-3} in the absence of a $Ni(OH)_2$ precipitate, it increases with increasing NaOH concentration. This is easily explained by the following facts. The amount of dissolved silica is comparable to the amount of Na^+ ions,[1] and the solubility of silica steeply increases with increasing the pH of the solution at pH $>$ 8.[2] Therefore, the difference in the amount of dissolved silica between the presence and absence of $Ni(OH)_2$ can be regarded as silica loading on $Ni(OH)_2$ (Fig. 1). In the case of SiO_2–ZrO_2,[4] we confirmed that the difference was comparable to the silica loading measured by using ICP-AES.

The increases in silica loading with the HT period within 150 h (Fig. 2) indicate that the SiO_2 species dissolved from the glass successively deposits on the $Ni(OH)_2$ precipitate under the HT conditions at 100 °C. The deposition rate is fast at a high NaOH concentration because of the high silica solubility. In the preparation of SiO_2–ZrO_2,[4] we considered that the dissolution of SiO_2 from SiO_2–ZrO_2 scarcely proceeded because a SiO_2–ZrO_2 composite had a high alkali resistance.[17] In a similar manner, the reverse reaction, the dissolution of SiO_2 from SiO_2–$Ni(OH)_2$, hardly proceeds in the present SiO_2–NiO system. The formation of the Ni_2SiO_4 phase observed in the SiO_2–$Ni(OH)_2$ samples (Fig. 6) is one of the reasons why the reverse reaction hardly occurs. It is probable that the Ni_2SiO_4 phase is undissolved in the HT process. Above silica loading of ca. 300 mg g_{NiO}^{-1}, however, further silica deposition dose not occur on the SiO_2–$Ni(OH)_2$ at any NaOH concentration (Fig. 2). This indicates that a meta-stable structure is attained in the dissolution-deposition process. In other words, the SiO_2–$Ni(OH)_2$ surface with the maximum silica loading becomes the same surface as pure silica with respect to the solubility. A similar saturation in silica loading was observed in the vapor-phase deposition of silica from tetraethoxysilane on alumina.[5,6]

Agglomeration of $Ni(OH)_2$ and NiO Particles. In an XRD measurement (Figs. 6 and 7), the core $Ni(OH)_2$ crystallites were transformed into NiO during calcination at 500 °C, together with a change in the shape of the crystallites. A part of the deposited silica was detected as nickel silicate unreduced in H_2 at 500 °C (Fig. 7E), which agrees well with the TPR results (Fig. 9). Although Na_2SiO_3 was observed in a sample reduced at 800 °C with the transformation of Ni_2SiO_4 into the Ni metal phase (Fig. 7F), Na_2SiO_3 is not assumed to be the deposited silicate species. Burattin et al.[18] have reported a similar deposition of silicate: nickel phyllosilicate deposited on silica through dissolution-deposition of silica in an aqueous ammonia solution during homogeneous precipitation of the Ni(II) phase on silica using urea at 90 °C.

The XRD of SiO_2–$Ni(OH)_2$ (Fig. 6) suggests that the samples have strong anisotropy. At a high NaOH concentration, the anisotropy was retained during the HT process, while the anisotropy decreased with increasing HT period at a low concentration. The size and shape of $Ni(OH)_2$ crystallite varied in the HT process (Table 2 and Fig. 8).

It is probable that the formation of a pore structure is attributed by the agglomeration of $Ni(OH)_2$ in the HT process at 100 °C. The agglomeration state in SiO_2–coated samples is fixed during calcination because the pore-size distribution of SiO_2–NiO is similar to that of SiO_2–$Ni(OH)_2$. The pore-size distribution of SiO_2–NiO shifts to a large pore size with increasing HT period at a high concentration of NaOH (Fig. 5). This indicates that the agglomeration degree of SiO_2–$Ni(OH)_2$ particles varies in the HT process: the primary SiO_2–$Ni(OH)_2$ particles agglomerate loosely at high NaOH concentration. The agglomerates of SiO_2–$Ni(OH)_2$ are retained without sintering during calcination, whereas the shape of the core particles changes from rod to sphere. In contrast, a pure $Ni(OH)_2$ pre-

cipitate readily aggregates during the HT process in the absence of silica glass at 100 °C (Fig. 3), and is readily sintered during calcination (Fig. 4). A similar trend has been observed in pure ZrO_2; the SA of a $ZrO(OH)_2$ sample dried at 110 °C decreased from 220 to 90 $m^2\ g^{-1}$ with increasing the HT period from 0 to 192 h.[4]

It is obvious that a large difference in SA is found in samples prepared at different NaOH concentrations (Figs. 3 and 4). In samples prepared in a NaOH solution at 0.02 mol dm^{-3}, the SA value of SiO_2–$Ni(OH)_2$ was minimized at a HT period of 48 h, while the SA of SiO_2–NiO increased with increasing HT period, and decreased slightly through a maximum. The aggregation proceeded during calcination for a short HT period because the SA of SiO_2–$Ni(OH)_2$ is higher than that of SiO_2–NiO. For a long HT period, however, the deposited silica could be attributed to the high SA.

The high SA values of SiO_2–$Ni(OH)_2$ prepared at 0.5 mol dm^{-3} are unchanged in the HT process, whereas those at 0.02 mol dm^{-3} vary greatly with the HT period (Fig. 3). The facts can be explained by the difference in the deposition rate. We can say that the $Ni(OH)_2$ precipitate aggregates before sufficient silica deposits at a low NaOH concentration, while silica deposits before the $Ni(OH)_2$ precipitate aggregates at a high concentration. At a high NaOH concentration, the deposition rate is fast (Fig. 2), and a high SA of as-dried precipitate containing silica is maintained after calcinations (Fig. 4); a sufficient amount of silica deposition prevents NiO particles from aggregation during calcinations. Chuah and Jaenicke have reported similar changes in the SA of zirconia aged in different NaOH concentrations.[19]

Reduction Behavior of SiO_2–NiO. The structure of SiO_2–NiO seems to be aggregates of NiO cores covered with nickel silicate and/or silica shell. Although the nickel silicate species is not reduced by hydrogen at 500 °C, the core NiO is not protected by the silicate shell during the reduction; a part of the NiO in the samples is reduced, as shown in Fig. 7E. However, the irreducible nickel silicate and NiO are reduced at temperatures higher than 500 °C in the TPR profiles (Fig. 9). The TPR results show that the amount of irreducible nickel silicate increases with increasing silica loading. They also indicate that nickel silicate readily forms at a high NaOH concentration in the HT process. A nickel phyllosilicate deposited on silica reported by Burattin et al. was reduced at ca. 500 °C,[18] which is higher than that of pure NiO.

The Ni metal surface area of a sample reduced at 500 °C is at most 22 $m^2\ g^{-1}$ (Fig. 10), and is less than 30% of the total SA value (Fig. 11). The fraction of Ni metal surface decreases with increasing silica loading and NaOH concentration in the HT process. Since the densities of NiO and Ni metal are 6.72 and 8.90 g cm^{-3},[20] their molar volumes were calculated to be 11.1 and 6.59 $cm^3\ mol^{-1}$, respectively. This means that the average radius of Ni particle decreases to 84% of that of the original NiO particle during reduction, assuming that the particles are spheres. Thus, a NiO core particle contracts into a small Ni particle during reduction. Also, the molar volume of $Ni(OH)_2$ is calculated to be 22.6 $cm^3\ mol^{-1}$ using a density of 4.1 g cm^{-3}.[20] Because the average radius of the NiO spherical particle is 79% of that of $Ni(OH)_2$, a $Ni(OH)_2$ core particle also shrinks into a small NiO particle during calcination.

It is speculated that the nickel silicate shell that covered the $Ni(OH)_2$ core is broken during the calcination of SiO_2–$Ni(OH)_2$, and that the NiO surface is exposed. Thus, the exposed NiO is readily reduced at 500 °C. At a low NaOH concentration in the preparation, the $Ni(OH)_2$ precipitate aggregates during the gradual silica deposition. Because a large $Ni(OH)_2$ particle greatly decreased in volume during calcination and reduction, the exposed Ni surface could increase due to disintegration of the core-shell structure induced by the great volume change. On the other hand, at a high NaOH concentration, silica deposits quickly before $Ni(OH)_2$ precipitates aggregate. The resulting SiO_2–NiO particle is small, but has a small change in the core-shell structure during calcination. Thus, it has a small fraction of the Ni surface exposed after reduction. This consideration is supported by the difference in the silica deposition rate during the HT process.

Conclusions

Fine particles of SiO_2-coated NiO were prepared by depositing silica on the $Ni(OH)_2$ precipitate through a dissolution-deposition of silica under hydrothermal conditions in different concentrations of an aqueous NaOH solution with several pieces of silica glass tubes at 100 °C. A silica component dissolved from the silica glass was deposited on a fresh precipitate of $Ni(OH)_2$, and the silica loading increased with increasing the hydrothermal period. The specific surface area of the resulting SiO_2–NiO exceeded 200 $m^2\ g^{-1}$ even after calcination at 500 °C. In contrast to the fact that the primary particles of the pure $Ni(OH)_2$ readily aggregates, the silicate species deposited on the surface of $Ni(OH)_2$ particles prevents the agglomeration of the primary particles during calcination and reduction.

At a high NaOH concentration, silica deposits quickly before $Ni(OH)_2$ precipitate aggregates. The resulting SiO_2–NiO particles are small, but have a small change in the core-shell structure during calcination and reduction. On the other hand, at a low NaOH concentration in the preparation, the $Ni(OH)_2$ crystallites grow during gradual silica deposition, so that a relatively large NiO core particle decreases in volume during reduction. Disintegration of the core-shell structure induced by the great volume change could expose the Ni surface to a large extent. Consequently, the reduced SiO_2–NiO has a Ni metal surface area as high as 22 $m^2\ g^{-1}$ after reduction at 500 °C.

The authors wish to thank Mr. Hiroki Sugiyama, graduate students of Chiba University, for measuring some preliminary data.

References

1 R. K. Iler, "The Chemistry of Silica," Wiley, New York (1979), p. 30.

2 P. W. J. Wijnen, T. P. M. Beelen, J. W. de Haan, C. P. J. Rummens, L. J. M. van de Ven, and R. A. van Santen, *J. Non-Cryst. Solids*, **109**, 85 (1989).

3 J. J. Mazer and J. V. Walter, *J. Non-Cryst. Solids*, **170**, 32 (1994).

4 S. Sato, R. Takahashi, T. Sodesawa, S. Tanaka, K. Oguma, and K. Ogura, *J. Catal.*, **196**, 190 (2000).

5 S. Sato, M. Toita, Y. Q. Yu, T. Sodesawa, and F. Nozaki, *Chem. Lett.*, **1987**, 1535.
6 S. Sato, M. Toita, T. Sodesawa, and F. Nozaki, *Appl. Catal.*, **62**, 73 (1990).
7 S. Sato, T. Sodesawa, F. Nozaki, and H. Shoji, *J. Mol. Catal.*, **66**, 343 (1991).
8 T. Jin, T. Okuhara, and J. M. White, *J. Chem. Soc., Chem. Commun.*, **1987**, 1248.
9 M. Niwa, N. Katada, and Y. Murakami, *J. Catal.*, **134**, 340 (1992).
10 G. A. Park, *Chem. Rev.*, **1965**, 177.
11 D. Dollimore and G. R. Heal, *J. Appl. Chem.*, **14**, 109 (1964).
12 T. Nakayama, N. Ichikuni, S. Sato, and F. Nozaki, *Appl. Catal. A*, **158**, 185 (1997).
13 S. Sato, R. Takahashi, T. Sodesawa, K. Yuma, and Y. Obata, *J. Catal.*, **196**, 195 (2000).
14 S. Sato, R. Takahashi, T. Sodesawa, F. Nozaki, X.-Z. Jin, S. Suzuki, and T. Nakayama, *J. Catal.*, **191**, 261 (2000).
15 R. Takahashi, S. Sato, T. Sodesawa, M. Kato, and T. Yoshii, *Chem. Lett.*, **1999**, 305.
16 N. Nakamura, R. Takahashi, S. Sato, T. Sodesawa, and S. Yoshida, *Phys. Chem. Chem. Phys.*, **2**, 4983 (2000).
17 L. J. Larner, K. Speakman, and A. Majumdar, *J. Non-Cryst. Solids*, **20**, 43 (1976).
18 P. Burattin, M. Che, and C. Louis, *J. Phys. Chem. B*, **102**, 2722 (1998).
19 G. K. Chuah and S. Jaenicke, *Appl. Catal. A*, **163**, 261 (1997).
20 "Handbook of Chemistry and Physics" 79th ed by D. R. Lide CRC Press, Boca Raton, FL (1998).